ROBUST TRANSMISSION OF COMPRESSED IMAGES OVER NOISY GAUSSIAN CHANNELS

Thomas P. O'Rourke, Robert L. Stevenson, Yih-Fang Huang,
Lance C. Perez and Daniel J. Costello Jr.

Laboratory for Image and Signal Analysis
Department of Electrical Enginering
University of Notre Dame
Notre Dame, IN 46556 USA

ABSTRACT

Many image communication systems have constraints on bandwidth, power and time which prohibit transmission of uncompressed raw image data. Compressed image formats, however, are extremely sensitive to bit errors which can seriously degrade the quality of the image at the receiver. A new list-based iterative trellis decoder is proposed which accepts feedback from a post-processor which can detect channel errors in the reconstructed image. Experimental results are shown which indicate the new decoder provides significant improvement over the standard Viterbi decoder.

1. INTRODUCTION

The sensitivity of the compressed image representation to bit errors requires application of a channel code before transmission over noisy channels. To prevent the uncontrolled degradation caused by a channel error, an error controlling channel code is applied to the compressed representation before transmission. The cost of the additional bits for redundancy in the channel code is paid for by an increased compression ratio which results in additional controlled quantization error.

Although the channel code greatly reduces the number of errors in the compressed image representation, a single error could still produce severe degradation in the quality of the received image. The post-processing method for reducing the visibility of quantization errors presented in [1, 2] makes use of the Huber Markov random field (HMRF) image model. The robust image communication system proposed here uses this image model to detect errors in the compressed image representation and feeds this error information back to the channel decoder for a second pass at decoding the channel symbols. After channel errors have been corrected, the image is post-processed to reduce the visibility of the quantization error. Unlike other algorithms, this system coordinates channel error recovery with quantization error reduction. A new iterative channel decoder accepts error feedback from the now dual-purpose post-processor. In Section 2, a more detailed summary of the proposed image communication system will be presented.

Experimental results are shown in Section 3 to illustrate the concepts involved. The results of simulation experiments also show the average performance of the proposed system for varying noise levels.

2. SYSTEM SUMMARY

A block diagram of the proposed image communication system is shown in Figure 1.

2.1. Transmitter

The input image i is compressed by the source encoder using the JPEG still image compression standard [3]. JPEG's extended sequential mode of operation is used with custom quantization tables, optimized Huffman coding tables, and restart markers after each row of blocks. The restart markers limit the influence of a channel error to a single row of blocks. The compressed representation b is encoded for the noisy channel using a rate 1/2 convolutional code with constraint length 7 [4]. The bit sequence b^* is then transmitted over the noisy channel using BPSK modulation.

2.2. Receiver

An iterative decoder based on a soft decision Viterbi trellis decoder interprets the noisy received bit-stream $\hat{b}^*$. The first iteration decodes the standard soft decision trellis to obtain the maximum likelihood sequence $\hat{b}$ given the received channel symbols. However, it is also known that $\hat{b}$ is a JPEG compressed image representation. Since a correct decoding of the JPEG header information is critical to the correct reconstruction of the image, the second iteration redecodes the section of the trellis containing the JPEG header. The header syntax defined by the JPEG standard determines the value of many bits in the header and allows detection of incorrect header information. The known bits reduce the number of paths through the trellis and decrease the probability of decoding an incorrect path. This is very similar to the pinned state decoder described in [5].

The third iteration considers the header to be known correctly and redecodes sections of the trellis corresponding to entropy coded image data which have been signaled by the post-processor as possible sites for error events. The
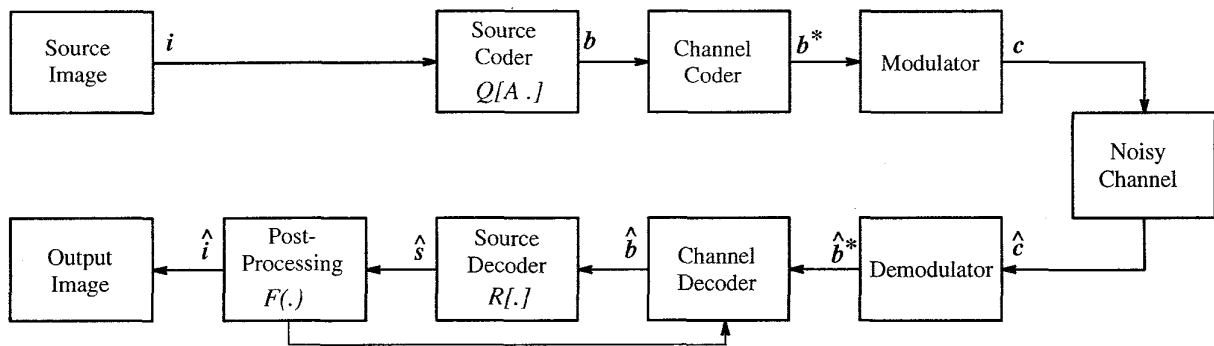
Figure 1: Proposed image communication system

success of the third iteration depends on the ability of the post-processor to detect error events in the reconstructed image. The errors are detected using the Huber-Markov random field (HMRF) image model. See [1, 2] for more information on the HMRF image model. The HMRF model is characterized by a special form of the Gibbs distribution

$$Pr(\mathbf{x}) = \frac{1}{Z} \exp\{-\frac{1}{\lambda} \sum_{c \in C} \rho_T(\mathbf{d}_c^t \mathbf{x})\}$$

where λ is a scalar constant that is greater than zero, $\mathbf{d}_c$ is a collection of linear operators and the function $\rho_T(\cdot)$ is given by

$$\rho_T(u) = \left\{ \begin{array}{ll} u^2, & |u| \leq T, \\ T^2 + 2T(|u| - T), & |u| > T. \end{array} \right.$$

This model is used to detect errors in a region of the image by estimating the probability of that region. Regions which are greatly affected by channel errors will have a large value for the exponent term $\sum_{c \in C} \rho_T(\mathbf{d}_c^t \mathbf{x})$ and the probability measure for these regions will be very low.

An error event produces three different types of artifacts in the reconstructed image. A missed End-of-Block code will cause an incorrect number of blocks for a particular row. While an incorrect number of blocks indicates an error has occurred, this first type of error does not provide information on where in the row the error occurred. Second, an error in the DC term will propagate until the next restart marker at the end of the row. This error can be detected by calculating the probability from the image model for the boundary area between the current row and the previous row. The third type of error occurs in the AC coefficients and often causes a single 8×8 block to differ greatly from the blocks expected by the image model. This error is detected by calculating the image model on each 8×8 block and is most easily detected when large high frequency components are present. This third type of error is most useful since the location of the error within the row can be calculated. The first and last bits of the row are indicated by restart markers. The region of doubt is calculated as $\pm 10\%$ of the bits in the row and is centered at the estimated position of the low-probability block in the bit-stream. Since error events from the channel decoder can produce a burst of errors, a combination of these three types of artifacts are often found together.
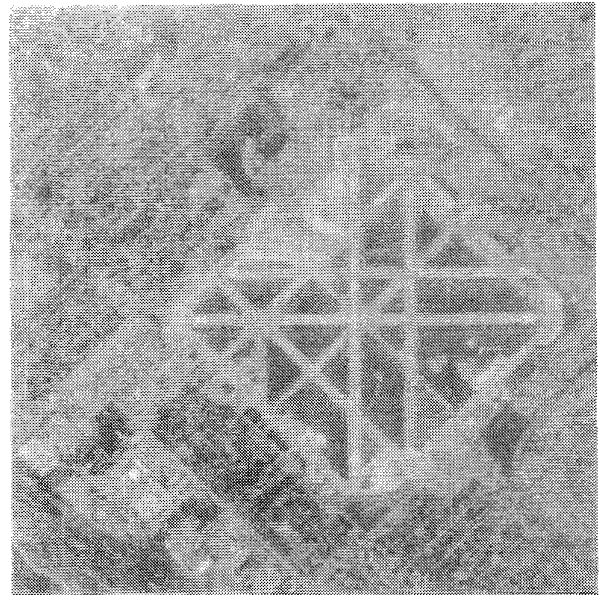

Figure 2: Original airport image, 256×256.

Information about possible error locations is fed back to the trellis decoder for reconsideration. Boundaries between rows and individual blocks which have probabilities below a particular error detection threshold are considered possible error regions and the corresponding sections of the bit-stream are marked. To prevent false alarms, the locations of the three 8×8 image blocks with the lowest probability are given to the decoder as side information. Additionally, the error detection threshold which is calculated for the particular image is also given to the decoder as side information. This small amount of side information can be included in the header with additional redundancy for error protection.

The Viterbi decoder makes a branch decision at each state to select the incoming path with the lowest weight. When the post-processor questions the decoding of the trellis, the confidence with which each branch decision is made is entered into a list for each state along the most likely path in the region of doubt. This list is sorted with the least confident decision at the top. The branch decision with
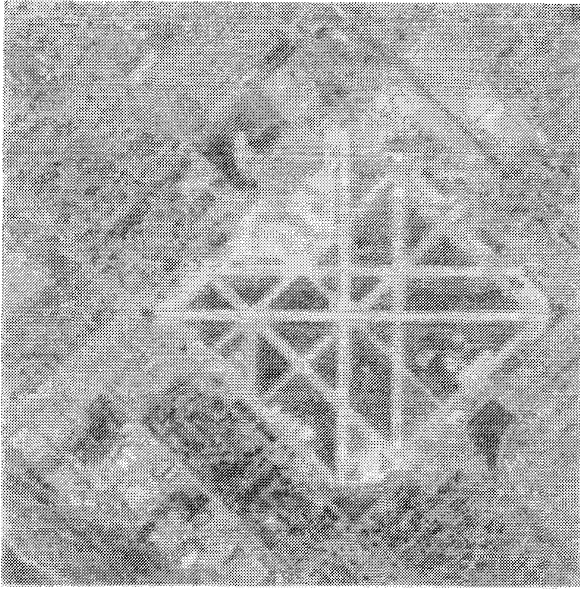
Figure 3: Airport image compressed by JPEG to 1.00 bpp, no errors.
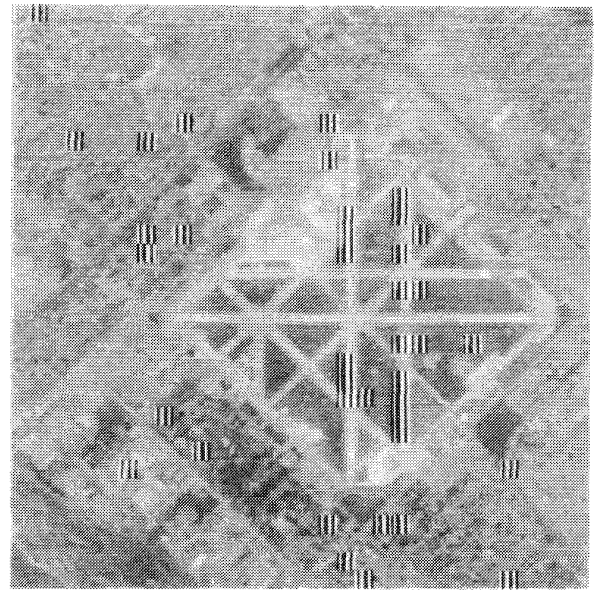

Figure 4: Example of quantization table error, after first iteration, Channel SNR 3.60 dB.

least confidence is overturned and the new path through the trellis is decoded, uncompressed, and sent to the post-processor. The process continues overturning branch decisions in the sorted list until the post-processor does not signal an error in this section or the end of the list is reached. Only one branch decision is overturned at a time since it is assumed the region of doubt contains only a single error event. To prevent erroneous redecoding due to false alarms signaled by the post-processor, the length of the list is limited to contain only branch decisions which were made with confidence less than a particular threshold value.

3. RESULTS

Experiments were run using the airport image shown in Figure 2. This image was compressed to 1.00 bpp, see Figure 3. Image SNR is used here to measure image quality. Although subjective image evaluation is more meaningful, an objective quality measure was needed to illustrate performance averaged over several trials. The compression reduces the image SNR to 23.29 dB. Channel SNR (E_p/N_0) is expressed in dB where E_p is the energy per pixel. Since the compressed image has 1.00 bpp, this is equal to the more common E_b/N_0 where E_b is the energy per information bit. Using E_p/N_0 will allow comparison of systems with different compression ratios.

The importance of correct decoding of the image header is shown in Figure 4. An error in the quantization table after standard Viterbi decoding has severely degraded the image (SNR 15.46 dB). This error is corrected in the second iteration. The resulting image (SNR 23.26 dB) contains only one small error which is not very noticeable and not detected in the third iteration.

Since the image header consists of a relatively small number of bits, most of the error events appear in the larger entropy coded image body. The features which make an error highly visible can be seen in Figure 5 which shows an example with two error events after the first iteration (SNR 19.18 dB). The effect of each channel error is limited to a single row by the restart markers. The first error event caused an extra block to be inserted shifting the row to the right. In the second error event, a missing End-of-Block code caused the next block to be treated as high frequency information which shifted the remainder of the row to the left. A DC error is also propagated through the rest of both rows. Both of these error events are corrected in the third iteration resulting in an image identical to the error free image shown in Figure 3. The quantization error reduction by the post-processor is not shown here.

While the above examples show very good error correction, the actual performance will vary depending on the particular realization of the noise. Different noise sequences of equal power can have very different effects on the reconstructed images. Figure 6 shows the average performance of the system under consideration. 600 trials were conducted for each of the nine channel SNR levels. As expected, the image SNR increases as the channel SNR increases. The quantization noise due to compression limits the performance at high channel SNR. Performance after standard Viterbi decoding, corresponding to the first iteration, is shown with the solid line. The dotted line shows performance after the second iteration has corrected header errors. The dashed line shows performance after the third iteration has corrected errors in the image body. Images which are severely degraded by header errors improve tremendously when the error in the header is corrected. Although more images have errors in the image body, the degradations which are corrected are less severe.
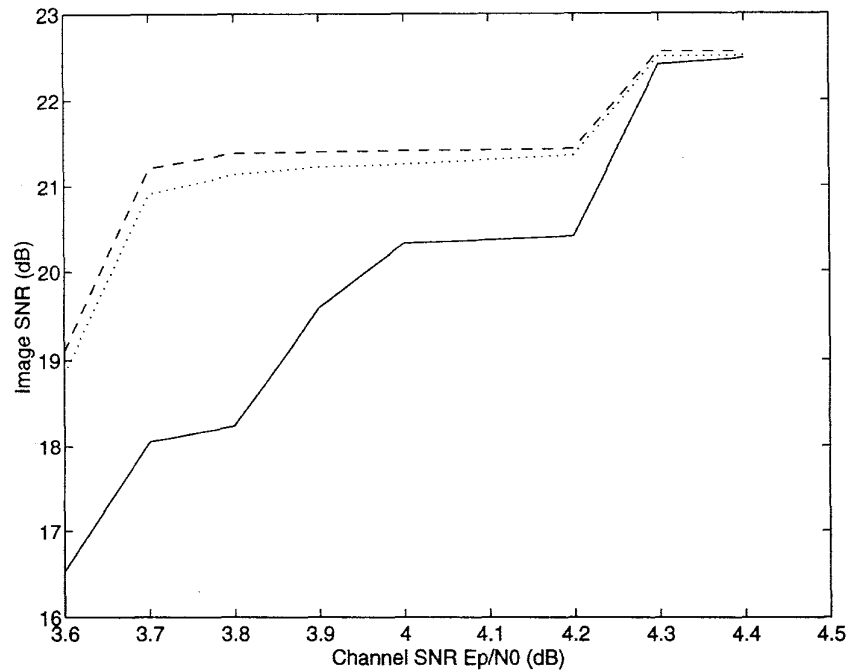
2321

Figure 6: Image SNR vs. Channel SNR

4. CONCLUSION

The new iterative trellis decoder is able to overcome channel noise using knowledge of compressed image syntax and the HMRF image model. The results are scalable to different degrees of quantization and can be extended to other compression techniques. Additional error protection is possible by using a longer constraint convolutional code at the expense of additional receiver complexity.

5. REFERENCES

[1] R. L. Stevenson, "Reduction of coding artifacts in transform image coding," in *Proc. ICASSP-93*, (Minneapolis, MN), pp. V:401–404, Apr. 1993.

[2] T. P. O'Rourke and R. L. Stevenson, "Improved image decompression for reduced transform coding artifacts," in *Proc. SPIE Image and Video Processing II*, vol. 2182, (San Jose, CA, Feb. 7-9, 1994), pp. 90-101, 1994.

[3] W. B. Pennebaker and J. L. Mitchell, *JPEG: Still Image Data Compression Standard.* New York: Van Nostrand Reinhold, 1993.

[4] S. Lin and D. J. Costello, Jr., *Error Control Coding: Fundamentals and Applications*, Englewood Cliffs, NJ: Prentice-Hall, 1983.

[5] O. Collins and M. Hizlan, "Determinate State Convolutional Codes," *IEEE Trans. on Communications*, vol. 41, pp. 1785-1794, Dec. 1993.
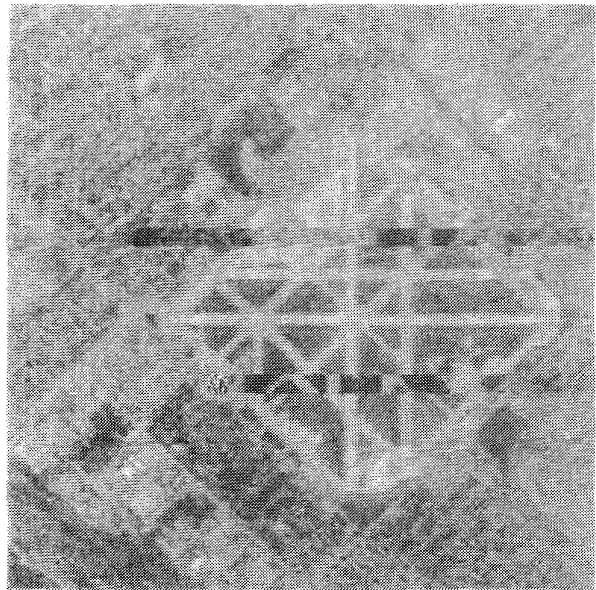
Figure 5: Example with 2 error events in entropy coded data, after first iteration, Channel SNR 3.60 dB.